International Journal of Modern Manufacturing Technologies
ISSN 2067–3604, Vol. XV, No. 2 / 2023
https://doi.org/10.54684/ijmmt.2023.15.2.91

CORROSION RESISTANCE OF COLD-ROLLED AISI 301 STAINLESS STEEL

Agnieszka Kurc-Lisiecka[1], Aleksander Lisiecki[2]

[1]WSB Merito University in Poznań, Faculty of WSB Merito University in Chorzów, Institute of Applied Sciences, Department of Logistics and Management Engineering, 29 Sportowa Str., 41-506 Chorzów, Poland
[2]Silesian University of Technology, Faculty of Mechanical Engineering, Department of Welding Engineering, Konarskiego 18A Str., 44-100 Gliwice, Poland

Corresponding author: Agnieszka Kurc-Lisiecka, agnieszka.kurc-lisiecka@chorzow.merito.pl

Abstract: The performed investigations concerned on the effect of cold rolling on the corrosion behavior and microstructure of austenitic AISI 301 stainless steel. Samples of steel strip were cold-rolled within the degree of deformation 30%, 50% and 80%. The corrosion resistance test was examined using gravimetric and potentiodynamic method. Corrosion tests were conducted in acidic and alkaline corrosive environments. A light microscope and a scanning electron microscope were used to observe the surface morphology of the samples after corrosion testing. Corrosion tests by gravimetric method showed that investigated steel is not resistant to corrosion in 0.5N H_2SO_4 solution, while no significant weight loss was observed in artificial seawater solution (0.5N NaCl). Based on potentiodynamic tests carried out in 0.5N NaCl solution, it was found that the pitting corrosion resistance of the tested cold-rolled steel AISI 301 decreases with an increase in the degree of plastic deformation in the range of 30% to 80%. However, a decrease in the corrosion potential and an increase in the current density were observed on the polarisation curves. The propensity of the steel to initiation and propagation pitting was found to increase both with increasing degree of deformation and the associated increase in the volume proportion of martensite-α' in the material structure. The occurring of martensite-α' in the investigated steel was confirmed by X-ray methods.
Key words: steel AISI 301, plastic deformation, cold rolling, corrosion resistance, microstructure, gravimetric and potentiodynamic method, pitting corrosion, general corrosion.

1. INTRODUCTION

Corrosion is defined as the destruction of a material under the influence of a chemical or electrochemical reaction with the surrounding environment. According to this general definition, corrosion applies not only to metallic materials, but to any type of material, such as ceramics, plastics, composites (Blicharski, 2004). Standard PN-EN ISO 8044:2020 provides a more extensive definition of this concept, according to which corrosion is a physicochemical interaction between a metallic material and its environment that results in changes in the properties of the metal, and that may lead to significant impairment of the function of the metal, the environment or the technical system, of which these form a part. The mechanism of corrosion of various materials depends on the type of electrical conductivity at the material-environment interface and the type of environment. For materials with high conductivity, corrosion is mainly electrochemical (wet corrosion). On the other hand, at low or no conductivity, corrosion occurs as a chemical or physicochemical process. Corrosion resistance of metals and alloys is associated with the formation of a nanometric, invisible layer on the surface of metal products, which protects the metal from corrosion. This phenomenon is called passivation of the metal surface, and the state in which the metal is in - the passive state. Passivation is marked by a change in the electrochemical potential of the metal to a more positive one. A significant tendency to passivation is shown by elements such as chromium and nickel, the main alloying additives to stainless steels. A chromium content of 12-18% in the steel causes it to exhibit a passivation capacity close to that of pure chromium. In turn, the addition of nickel to the steel, with the simultaneous presence of Mo, Si and Cu, causes stainless steels containing these elements to have very good corrosion resistance also in non-oxidizing environments, such as HCl. The passive oxide film formed on stainless steels is usually 1 to 10nm thick and can be damaged by mechanical or chemical interactions, so in order to effectively protect the metal, the steel should have the ability to rebuild (renew) the protective film in a given environment (Lamb, 2001, Darowicki, 2008). Progressive corrosion can cause a significant reduction in the mechanical and functional properties of machinery, equipment and components, such as: steam boilers, bridge structures, turbine blades, significantly reducing the safety of their use. It affects nearly 30% of the total number of products made of metals and their alloys (Dobrzański, 2009).

An important performance characteristic of austenitic steels is their significant resistance to various types of corrosion, such as: uniform corrosion in air, sweet water, organic acids, nitric acid solutions and alkaline solutions. The rate of uniform corrosion for metals or alloys at a level of no more than 0.15 mm/year allows them to be used for responsible parts of equipment exposed to corrosion damage, such as: valve seats of internal combustion engines or pump impellers. In seawater environments, the corrosion rate of austenitic steels does not exceed 2.5×10^{-5} mm/year. The degree of corrosion resistance is not the same for all austenitic steels and depends on the proportion of Cr and Ni. Among the most dangerous types of local corrosion that austenitic steels undergo are intergranular, pitting and stress corrosion cracking (Dobrzański, 2009, Lisiecki et al., 2019).

Intergranular corrosion is corrosion occurring at the boundaries of metal grains or in areas adjacent to them. In Cr-Ni stainless steels, this type of corrosion is associated with the phenomenon of the separation of chromium carbides ($M_{23}C_6$) at grain boundaries and the depletion of grain boundary areas in chromium. When the carbon content is higher than 0.03% there is a tendency for carbides to be separated during annealing in the temperature range of 500÷800°C. In order to prevent intergranular corrosion of stainless steels, the following methods are used: re-saturating from the temperature 1050◦C, the so-called stabilization of steel by introducing carbide-forming elements with a higher chemical affinity for carbon than Cr, most often Ti or Nb, which form permanent MX-type carbides, and reducing the C concentration of carbon in steel to less than 0.03% (Azambuja and Martini, 2003, Peğuet et al., 2007).

Pitting corrosion is localized corrosion that causes the formation of pits, or depressions that progress from the surface into the depths of the steel. In corrosion-resistant steels, this corrosion involves the formation of pits, initiated at the site of damage to the passive oxide layer, which can lead to complete perforation of thin-walled products (Dobrzański, 2009, Abreu et al., 2007). Pitting corrosion of stainless steels occurs most often in aqueous environments containing halide ions, i.e. Cl^-, Br^-, I^-. It usually appears on all kinds of internal (non-metallic inclusions, separations, deformations) and external metal inhomogeneities (edges, scratches, dents, scale residues, deposits, etc.). In contrast, smooth and homogeneous surfaces are far more resistant to this type of corrosion (Baszkiewicz and Kamiński, 1997, Pardo et al., 2007). A Pitting Resistance Equivalent (PRE) index is used for a relatively quick, though only approximate, assessment of the resistance of stainless steels to pitting corrosion. This index can take different formulas, but the most commonly used index is PRE in the following form:

$$PRE = \%Cr + 3.3\times\%Mo + 16\times\%N \quad (1)$$

The higher the PRE value, the greater the steel's resistance to pitting corrosion (Baszkiewicz and Kamiński, 1997).

The final shape of stainless steel products, semi-finished products, or components is obtained during plastic processing involving cold rolling or deep drawing. Therefore, the presence of strain martensite in Cr-Ni metastable steel grades is common. The appearance of α'-martensite changes the single-phase state of the steel, therefore physico-chemical properties of the steel also change. The α′ and γ phases have various corrosion potentials, that's why it simple for them to become the anode and cathode of a corrosion battery, respectively. Therefore, the corrosion resistance of metastable austenite stainless steel will decrease during cold working, because of an increase of dislocation density and occuring of deformation twins and also martensite-α' (Otero et al., 1995, Chunchun and Gang, 2004, Abreu et al., 2007, Kerner et al., 2007). Many authors have studied the impact of cold working on the corrosion behavior of steels 300-series (according to AISI), for example, in (Peguet et al. 11) the authors reported different roles of cold working on pitting corrosion resistance at different stages of pitting, including pitting initiation, propagation and repassivation. The authors suggested that at the initiation stage, a maximum of metastable pits is found for 10% tensile deformation or 20% cold-rolling reduction. This behaviour, have been seen even in ferritic grades, so contradicts the theory that strain-induced martensite is the main factor governing sensitivity to corrosion. On the other hand, regarding the propagation stage at mesoscopic scale, the highest pit dissolution rate is obtained for 20% cold-rolling reduction, when dislocations piled up on inclusions are believed to preferentially dissolve. In turne, the dissolution rate increases monotonously at the macroscopic propagation stage, when the overall density of dislocations is more probably the relevant factor. The authors were found that pitting potential (V_{pit}) combines in a single criterion both the resistance to pit initiation, pit propagation, and pit repassivation. In them work, V_{pit} more affected by the propagation/repassivation stages than by pit initiation and then vary monotonously with cold-rolling reduction. The authors of the publication (Barbucci et al., 2002) found that the passive currents of 304 stainless steel in sulfate and chloride media strongly increased with degree of plastic deformation in cold-working process. According to the authors, the increased susceptibility of the tested steel to pitting corrosion of the samples after cold rolling was related to the formation of more defective oxide during anodic oxidation. On the other hand, authors suggested that the higher amount of nonperfect oxide was related with formation of defect in steel grains as well as the increasing of amout of marteniste in the steel structure. The effect of phase transformation ($\gamma\rightarrow\alpha'$) and the presence of a marteniste α' on the susceptibility of 316 steel plates to pitting corrosion was carried out in work (Salomon and Salomon, 2010). According to the authors, an increase in the degree of

deformation causes a decrease in the resistance of the tested steel to pitting corrosion. Numerous corrosion pits were observed on the surface of the tested steel, which formed in privileged areas. These places are areas of occurrence of the martensite phase-α'. It was suggested that the martensitic transformation occurs gradually in the steel plate and therefore areas of two-phase structure with different hardness are formed on its surface. However, the zones with a martensite phase-α' are less resistant to pitting corrosion.
Since the effect of plastic deformation and the induced martensitic transformation (γ→α') in Cr-Ni steels is still not clearly defined, the purpose of this study is to analyze the corrosion resistance of AISI 301 steel cold plastic deformed at 30%, 50% and 80%.

2. MATERIAL AND EXPERIMENTAL PROCEDURE

The material for testing was AISI 301 stainless steel delivered as 2-mm thick sheet and containing 0.05 pct C, 17.71 pct Cr, 7.65 pct Ni, 1.17 pct Mn, 0.56 pct Si, 0.41 pct Mo, 0.018 pct P, 0.003 ptc S, 0.03 pct N_2 by weight. The sheets of steel with 2-mm thick were supersaturated in water after its austenitizing for 1 hour at a temperature of 1100˚C and then cold rolling in a multistage process to reduce the thicknes to 0.4 mm (Fig.1). Sheets of steel were rolled multiple time in the same direction and keeping the same side of the sheet. The scheme of the longitudinal rolling process of the tested AISI 301 steel have been presented in Table 1. The degree of deformation for investigated steel during the rolling process was determined alternatively, assuming no sheet expansion, based on relations given in publication (Kurc-Lisiecka, 2022).

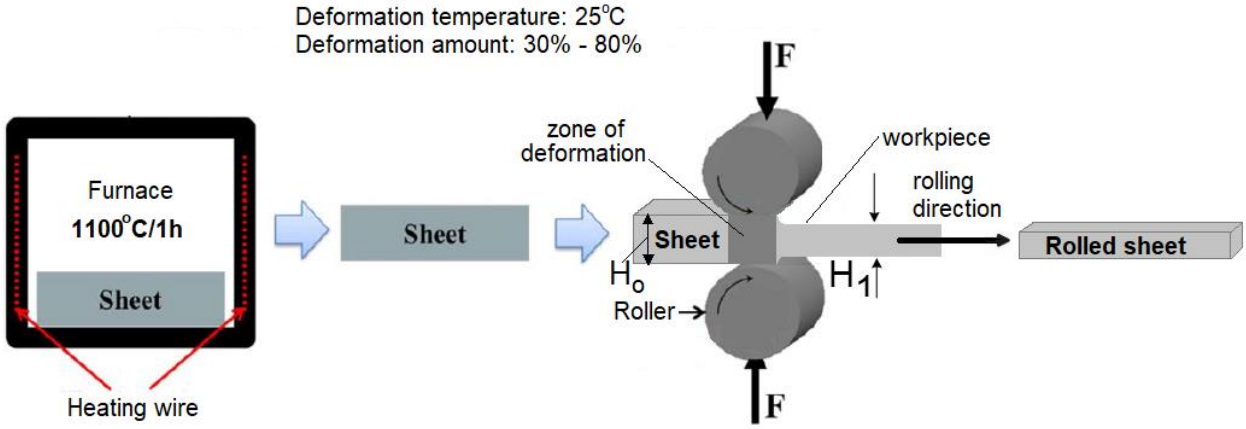

Fig. 1. Diagrammatic presentation of the deformation process for AISI 301 steel

Table 1. Schematic of the longitudinal rolling process for the tested AISI 301 steel

No.	Number of the culvert																	
	0	1	2	3	4	5	6	7	8	9	10	11	12	13	14	15	Deformation	
	Sheet thickness [mm]																Z_H [%]	ε_H
1	2.0	–	–	–	–	–	–	–	–	–	–	–	–	–			–	–
2	2.0	1.85	1.8	1.7	1.65	1.6	1.5	1.4	–	–	–	–	–	–			30	0.35
3	2.0	1.85	1.8	1.7	1.65	1.6	1.5	1.4	1.25	1.2	1.05	1.0	–	–			50	0.69
4	2.0	1.85	1.8	1.7	1.65	1.6	1.5	1.4	1.25	1.2	1.05	1.0	0.75	0.6	0.45	0.4	80	1.60

where: z_H – degree of deformation (draft), ε_H - logarithmic deformation

X-ray qualitative phase analysis of the tested AISI 301 steel specimens was carried out on an X-ray diffractometer type X'PERT PANalytical (PHILIPS), applying the filter radiation of an anode λCoKα (length was 0.179 nm). The data of the diffraction lines were recorded by "step-scanning" method in 2Θ range from 40° to 115° and the 0.02° step, the time of measurements amounting to 5s.
X-ray quantitative analysis were carried out on samples with dimensions 10×20 mm cut from AISI 301 steel in the as-delivered condition and after cold rolling with a draft of 30% to confirm the presents of the α'-martensite in steel structure. Diffractograms of the test samples were taken from the center layer of the steel sheets. Metallographic

observations of AISI 301 steel samples in the as-delivered (after solution heat treatment) and deformed state (30%) were performed on a LEICA MEF 4A light microscope, with magnification up to 400x.
Corrosion resistance of AISI 301 steel was examined using weight (gravimetric) and potentiodynamic methods.
Weight method. Corrosion tests were carried out in 0.5N NaCl and 0.5N H_2SO_4 solutions on samples with 20x15mm dimensions, according to the standard EN ISO 7384, EN ISO 8044 and EN ISO 3651-2. The specimens were cut along to rolling direction from steel sheet-metals in its delivery state and after cold rolling with a draft of 30%, 50% and 80%. Specimens were cleaned in 95.6% ethanol and they were weighed on analytical balance before starting the analysis. The solution temperature during the test was 23ºC±1ºC, while the test time was 25 days for 0.5N H_2SO_4 and 75 days for 0.5N NaCl, respectively. Initially, an identical exposure time (75 days) was assumed for steel specimens in both environments, but due to the corrosion destruction process being too fast for specimens immersed in 0.5N H_2SO_4, the time was shortened. Volume of corrosion loss, V_c, was calculated using the following dependence:

$$V_c = \frac{\Delta G}{A \cdot t}\left[\frac{g}{m^2 \cdot day}\right] \tag{2}$$

where: ΔG - mass loss of a sample [g], A - surface of a sample [m^2], t - time of the measurement [day].

Linear corrosion rate, V_p, was determined basing on the dependence:

$$V_p = V_c \cdot k\left[\frac{mm}{year}\right] \tag{3}$$

where: V_c - value of corrosion loss [$g/m^2 \cdot day$], *k* - ratio including mass loss of a sample and linear corrosion rate calculated by the formula: $k=365/1000 \cdot \rho$ where ρ - density of material, [g/cm^3].
For investigated AISI 301 steel the density of about $\rho=7.86$ [g/cm^3] was established.
The calculated weight loss of the sample should be compared with the value given in the standard (Table 2), and on this basis determine the group and scale of corrosion resistance of the AISI 301 steel.

Table 2. Part of the scale of corrosion resistance of metals according to PN-H-04608

Corrosion resistance group		Degree of corrosion resistance	Corrosion rate
Destignation	Marking		$V_p\left[\frac{mm}{year}\right]$
Completely resistant	I	1	< 0.001
Very resistant	II	2	0.001…0.005
		3	0.005…0.01
Resistant	III	4	0.01…0.05
		5	0.05…0.1
Less resistant	IV	6	0.1…0.5
		7	0.5…1.0
Slightly resistant	V	8	1.0…5.0
		9	5.0…10.0
Not resistant	VI	10	> 10.0

Potentiodynamic method. Corrosion tests were carried out in 0.5N solution of NaCl by recording anodic polarization curves according ASTM G5. Temperature of the solution during the test was equal 23ºC ± 1ºC. The VoltaLab® PGP 201 system for electrochemical tests was applied (Fig. 2).

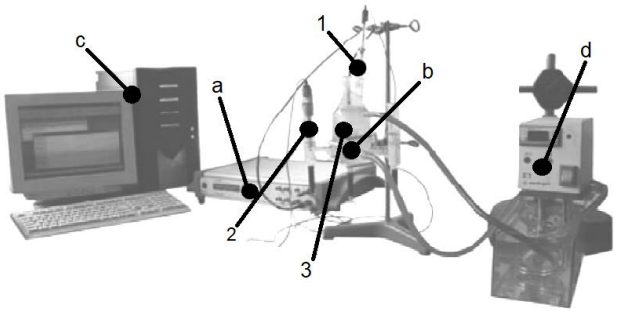

Fig. 2. Diagram of the corrosion resistance set, where:
a) potentiostat VoltaLab® PGP201, b) electrochemical cell: 1 – SCE electrode of KP-113 type, 2 – Pt electrode, 3 – sample, c) computer with VoltaMaster 4 software ver. 5.1, d) termostat Medlingen

Potentiodynamic test specimens prepared as 14.7 mm diameter disks were cut from AISI 301 steel in delivery state and after selected cold rolling reductions. The samples were cleaned in 95.6% ethanol before analysis. Tests were started from determination of E_{ocp} open circuit potential (to stable the experimental environment) and then anodic polarization curves with the potential range from -0.25 V_{SCE} to +1V_{SCE} in a scanned rate of 1mV/s. Each experiment was repeatedly conducted for many times with the same conditions to ensure the tests to be reproducible. In the potentiodynamic test the parameters such as corrosion potential (E_{cp}), current density (i_{cor}) were acquired by polarization plots and Tafel extrapolation method (Baszkiewicz and Kamiński, 1997, Varga et al., 2001). The i_{cor} represented the current in the middle of the passive region of the polarization plot.
The microscope observations of the surface samples subjected to corrosion resistance test in 0.5N NaCl and 0.5N H_2SO_4 solutions permitted to evaluate kinds and the rate of corrosion damages. In order to observe the morphology of the corrosion products formed on the material surface after weight loss tests the Scanning Electron Microscopy SUPRA^{TM}25 produced by ZEISS was used. Observations carried out applying the magnification of 280, 400 and 3000x.

3. RESULTS AND DISCUSSION

The AISI 301 stainless steel sheet in the delivery condition shows an austenite structure with an average grain size of about 19 μm, with annealed twins (Fig. 3a). The homogeneous austenite structure of the tested steel was confirmed by X-ray diffraction analysis (Fig. 3b).

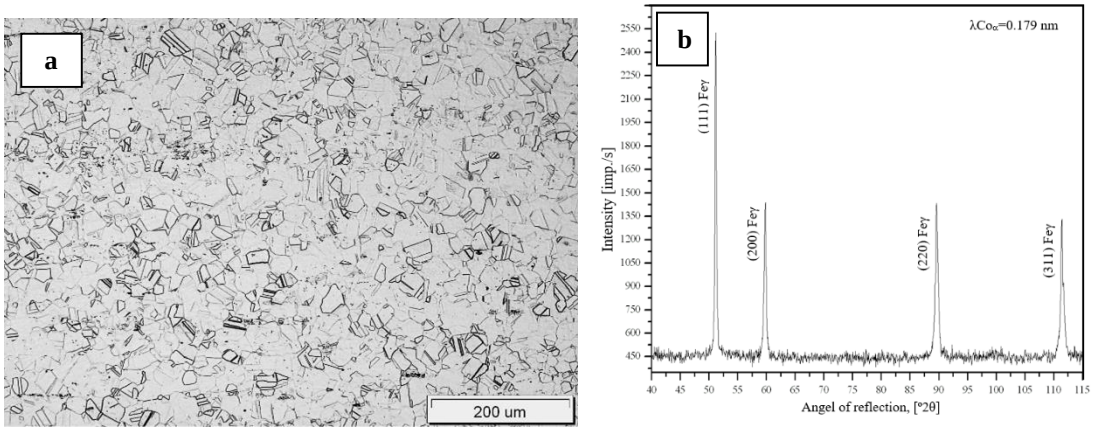

Fig. 3. Microstructure of AISI 301 steel in delivery state (a) and X-ray diffraction pattern (b)

In AISI 301 steel structure after 30% of deformation in cold rolling process metallographically distinctly elongated grains of the matrix γ could be detected with numerous effects of work hardening in the form of fine parallel and intersected lines and slip bands, as well as shear bands, which are sites of martensite-α' nucleation (Fig. 4a). It was also found that plastic deformation leads to a distinct elongation of the grains in the direction of rolling. The X-ray diffraction analysis confirm a two-phase structure (γ + α') of deformed AISI 301 steel. On the diffraction patterns of steel middle layers after 30% of cold rolling, there are disclosed six diffraction lines. Three of diffraction lines coming from planes (111)γ, (220)γ and (311)γ austenite phases and three (110)α', (200)α',

(211)α' reflection planes from martensite-α' phases (Fig. 4b). The diffractogram (Fig. 4b) shows only phases γ and α'. There is no peak indicating the presence of ε (hexagonal close packed, hcp) martensite. This means that ε martensite is or can be only a step of martensite transformation as suggested in work (Abreu, 2007). In this work probably the reaction γ→ε→α' has been completed because we start to investigated AISI 301 steel until after 30% of deformation, which is consistent with the results of work (Haušild et al., 2010). The author detected the ε-marteniste (hcp) phase in cold-rolled AISI 301 steel but in small deformation range (from 2.5% to 20%). So in this work the probably sequence of the martenisitic transformation is γ→α'.

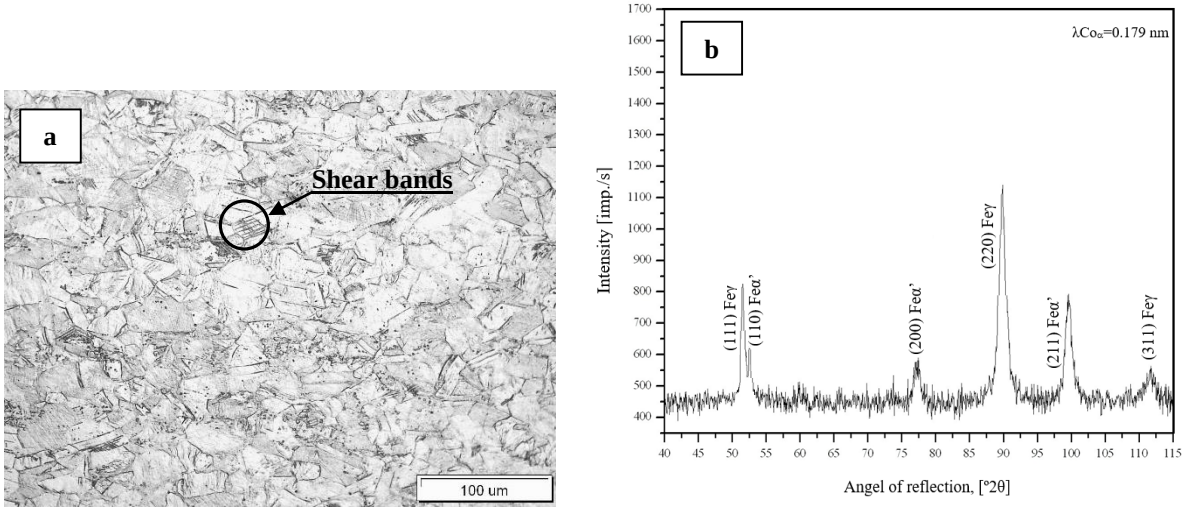

Fig. 4. Microstructure of AISI 301 steel after 30% of deformation (a) and X-ray diffraction pattern (b)

The calculate value of PRE for investigated AISI 301 stainless steel is about 19.5, which is in line with the range of PRE values adopted in the standard (17.5-19.5). It should be note, that in most cases, components for use in the oil and gas industries require a PRE greater than 32. For hydrogen sulphide (H_2S) environments and seawater service, a PRE of 40 or higher are typically used (steel grate 1.4410, 14507, 1.4501). Values of PRE also vary depending on the use environment. Corrosive media outside chlorides, service temperatures, component surface finishes, system design, and acidity can all further impact pitting resistance (BSAA, 2023).

Based on the corrosion test conducted in 0.5N H_2SO_4 solution, it was found that for AISI 301 steel in the delivery condition, the value of linear corrosion rate (V_p) was 4.0 $\left[\frac{mm}{year}\right]$, and the weight loss ($V_c$) was about 87 $\left[\frac{g}{m^2 \cdot day}\right]$. This means that AISI 301 steel is "slightly resistant" to this environment and, according to the PN-78/H-04608 standard, in the state of delivery it is characterized by an eighth degree of corrosion resistance. The results of corrosion tests on samples after plastic deformation in the range of 30% to 80% result in a slight deterioration of corrosion resistance, as marked by an increase in both the average V_p value to about 6.2 $\left[\frac{mm}{year}\right]$ and the average V_c value to about 140 $\left[\frac{g}{m^2 \cdot day}\right]$. Based on the calculated V_p values, as well as the Vc values, it was concluded that the tested steel is still included in the "sightly resistant" group, but shows a ninth degree of corrosion resistance. Cold-rolled samples were found to show slightly lower corrosion resistance in a 0.5N H_2SO_4. Corrosion tests in alkaline medium (0.5N NaCl) showed that the tested AISI 301 steel in the delivery condition has a value of linear corrosion rate (V_p) less then 0.001 $\left[\frac{mm}{year}\right]$, which indicates the "completely corrosion" of those materials (Ist degree of corrosion resistance, Table 2) in the tested environment. The results of corrosion testing of samples after plastic deformation in the range of 30% to 80% indicate that the average linear corrosion rate of AISI 301 steel is about 0.005 $\left[\frac{mm}{year}\right]$. Based on the calculated V_c values and in accordance with PN-78/H-04608, this steel is in the "very resistant" group, but is characterized by the IInd degree of corrosion resistance (Table 2). It was found that, cold deformed samples of AISI 301 steel have slightly lower resistance to corrosion in alkaline environment than the material in the as-delivered condition. For AISI 301 steel samples immersed in a chloride solution, the mass loss is more than 100 times lower despite three times longer exposure in this environment, compared to samples immersed in an acidic medium. The obtained results are consistent with those obtained for AISI 304 steel, as discussed in work (Štefec and Franz, 1978). This difference can be explained by the different course of

corrosion mechanisms. In acidic solutions, the corrosion process follows hydrogen depolarization, while in chloride media the samples corrode with oxygen depolarization. When hydrogen ion is depolarizer, as a result of the cathodic reaction, there is an increase in pH values in the immediate vicinity of the metal surface, and this usually initiates the course of side chemical reactions, such as precipitation on the surface of the metal insoluble metal hydroxides, or (when the pH increase is large enough) - chemical dissolution of the metal (Baszkiewicz and Kamiński, 1997).

In oxygen depolarization (corrosion in chloride solution), the O_2 included in the electrolyte is being reduced by electrons from the metal to hydroxide ions (OH^-), at the time on the steel surface appears a layer of corrosion products, protecting the material before further penetration of the corrosion medium, which is the reason for the lower mass loss of the sample in the alkaline solution compared to acidic environment. The uptake of chloride iron (Cl^-) take place in less corrosion-resistant areas (e.g., with non-metallic inclusions), where the potential differences occured. The taken up Cl^- form chlorine oxides of increased solubility, which causes local damage to the layer of corrosion products and the start of the formation of corrosion pits. The further spread of corrosion pits proceeds autocatalytically (Ozgowicz, et al., 2013).

In investigated AISI 301 steel in non-deformed state many micropores, corrosion pits and craks along the whole specimen surface were observed after immersed in 0.5N H_2SO_4 (Fig.5).

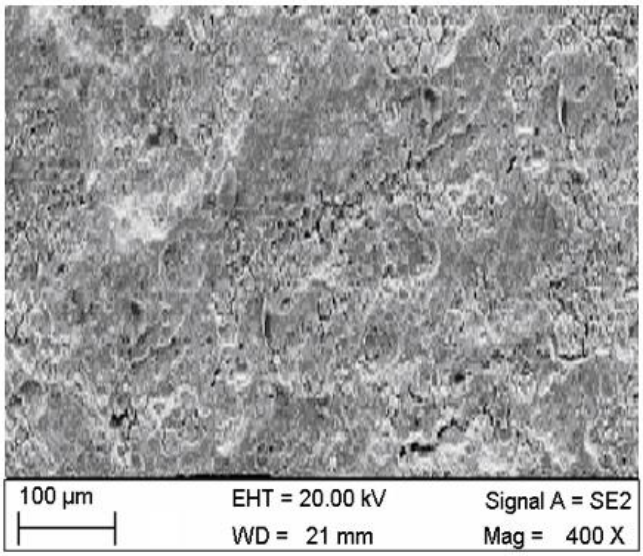

Fig. 5. Micropores, cracks and corrosion pits on the AISI 301 steel surface in a delivery state after immersion tests in 0.5N H_2SO_4 solution

Similar, though slightly smaller, corrosion pits are formed in the samples after immersion in 0.5N NaCl (Fig.6). It was found that the largest number of corrosion pits are formed at the locations of concentrations of non-metallic inclusions, as they are considered to be privileged for the formation of corrosion effects (Abreu et al., 2007).

After cold working with the deformation amount from 30% to 80% and subsequent immersion tests in 0.5N H_2SO_4 the AISI 301 steel shows a meaningful percentage mass decrement up to 60%. It was found that plastic deformation in cold working process causes the increase of the mass loss in acidic media in comparison with the specimens investigated in the non-deformed state. The morphology of a surface of the cold deformed AISI 301 steel samples after exposition in acidic media showed a various character of corrosion products (Figs. 7-9).

On AISI 301 steel surface after 30% of deformation and immersion in the 0.5N H_2SO_4 many corrosion pits of various size can be observed (Fig.7).

In the samples after 50% of cold deformation wide pits and micropores can be seen (Fig.8). The amount and the size of pits are very high and they are formed along the entire surface of specimens. Privileged places for pits forming are surface concentrations of non-metallic inclusions, which are also probable places of H_2 penetration.

After maximum, 80% of deformation on the AISI 301 steel surface the many number of corrosion pits, micropres a cracked passive layer (Fig.9). In case of corrosion test in acid medium deeper penetration of hydrogen can be occur, probably by martensite-α' laths – accumulating in a surroundings of non-metallic sulfide inclusions (Garcia et al., 2010). Literatura data shows (Abreu et al., 2007; Singh and Ray, 2007), that usually, the places of hydrogen accumulation are non-metallic inclusions, grain boundary areas and/or twin boundaries (Abreu et al., 2007; Singh & Ray, 2007).

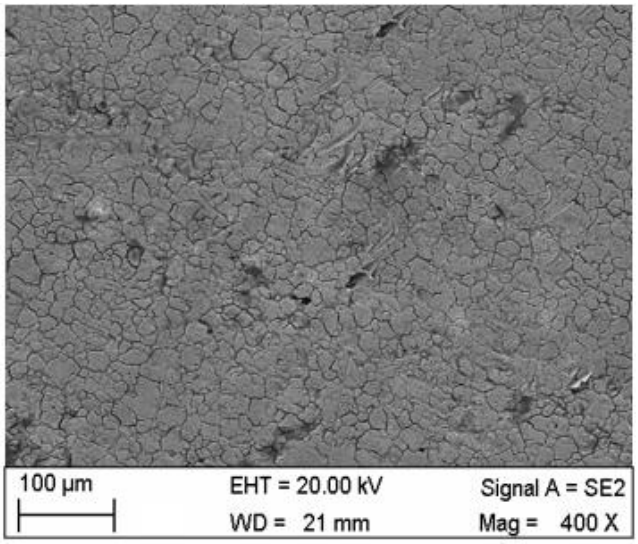

Fig. 6. Corrosion pits and the cracked surface layer of the AISI 301 steel in a delivery state after immersion tests in 0.5N NaCl solution

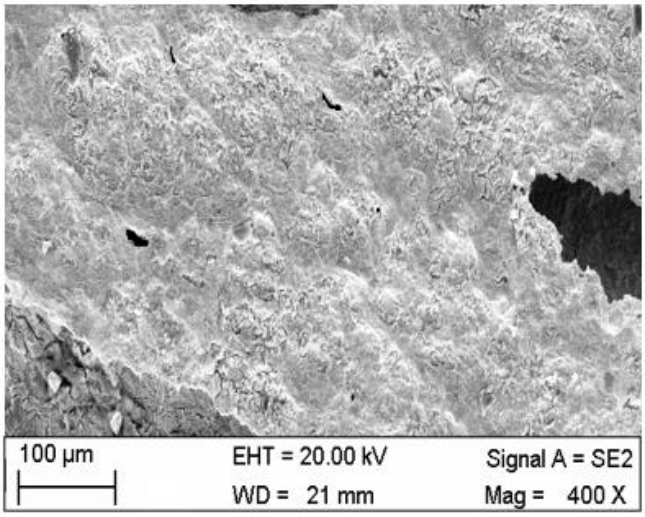

Fig. 7. Micropores, cracks, corrosion pits and the cracked surface layer of the AISI 301 steel 30% deformed and immersed in 0.5N H_2SO_4 solution

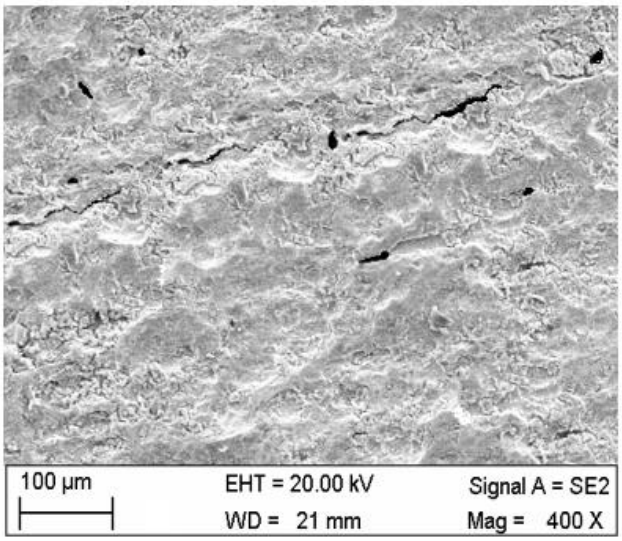

Fig. 8. Micropores, cracks and corrosion pits and the cracked surface layer of the AISI 301 steel 50% deformed and immersed in 0.5N H_2SO_4 solution

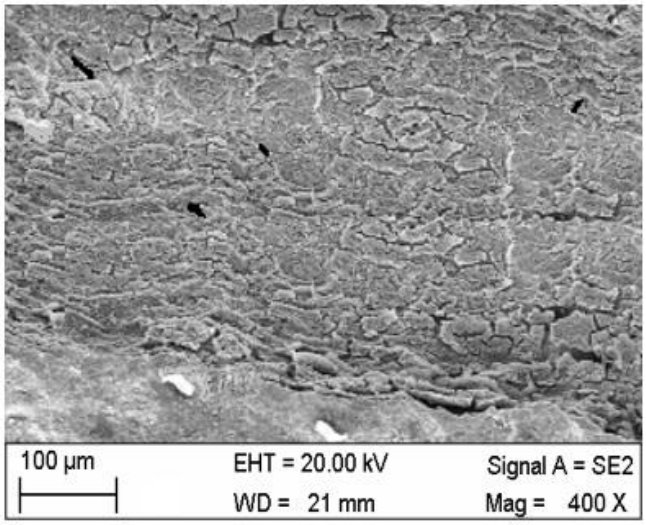

Fig. 9. Micropores, cracks, corrosion pits and the cracked passive layer of the AISI 301 steel 80% deformed and immersed in 0.5N H_2SO_4 solution

Comparison of the SEM images shows that there is a similarity in the trends of the pit density and mass loss. Especially in case of AISI 301 steel immersed in acid, an increase in deformation caused the introduction of defects in the material, which are preferred regions for the occurrence of pitting. Those observations are in the agreement with work (Silvia et al., 2023).

On the AISI 301 steel surface after immersion tests in 0.5N NaCl solution for 75 days the numerous pits and micropores of diversified size were observed (Figs. 10-13). It should be note, that the pits ocurrs on the surface of deformed samples (Figs. 10-12) have much bigger sizes than the pits observed on non-deformed samples (Fig.6). The paper (Chunchun and Gang, 2004) confirmed the presence of corrosion pits in a chloride environment. In addition, the authors found that the martensite phase destroys the integrity and compactness of the passive layer. For these reasons, the propagation of pitting in type 304 stainless steel was accelerated as the martensite content increased.

After cold working with the deformation amount from 30% to 80% and subsequent immersion tests in chloride environment AISI 301 steel shows many corrosion pits, micropores and cracked passive layer (Figs. 10-12). It should be note, that around the formed pits a damaged of superfical layer occured (Fig. 12).

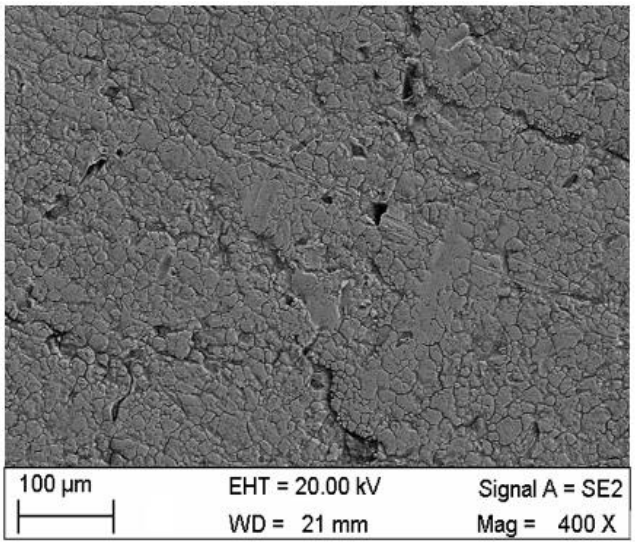

Fig. 10. Corrosion pits, micropores and the cracked surface layer of the AISI 301 steel 30% deformed and immersed in 0.5N NaCl solution

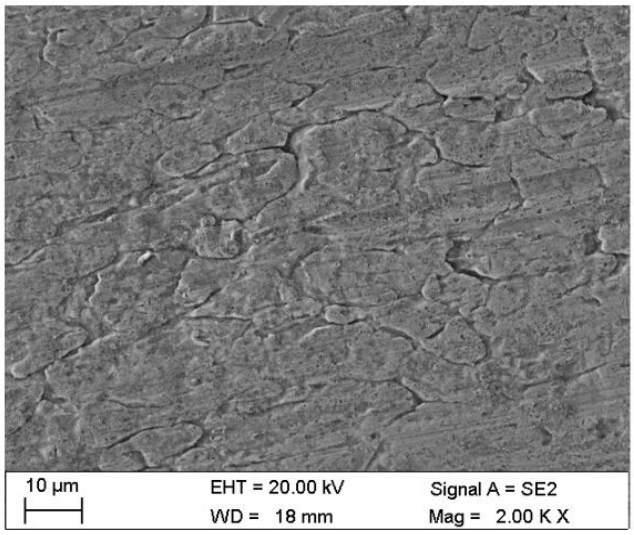

Fig. 11. Cracked surface layer, micropores and corrosion pits of the AISI 301 steel 50% deformed and immersed in 0.5N NaCl solution

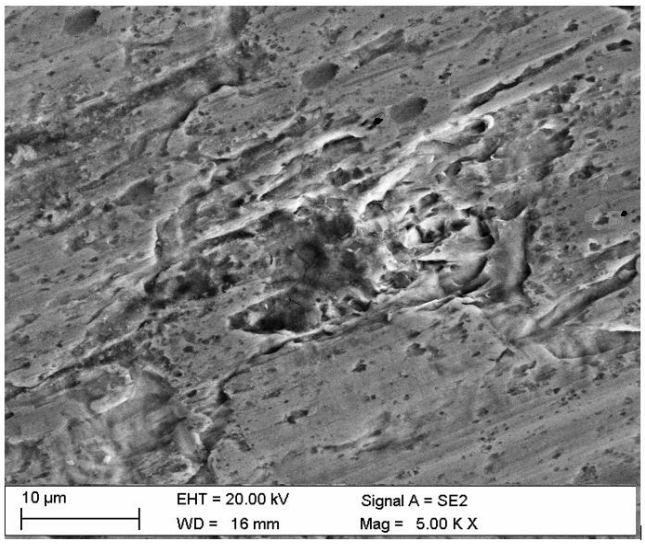

Fig. 12. Corrosion pits and micropores of the AISI 301 steel 80% deformed and immersed in 0.5N NaCl solution

Metallographic observations of surface of AISI 301 steel samples after corrosion tests in 0.5N NaCl showed numerous corrosion damages as well as the traces of intercrystalline corrosion running by the borders of grains. The numerous pits with effects of cold rolling are also visible (Figs. 12-15). Similar observations were made by the authors (Sing and Ray, 2007).

Based on SEM observations of plastically deformed specimens after corrosion testing, it was found that plastic deformation causes a significant acceleration of the corrosion process. It was further found that an increase in the degree of cold deformation from 30% to 80% leads to an increase in the number, size and depth of corrosion pits fulfilling the function of a local anode.

Performed electrochemical analysis in 0.5N NaCl revealed for investigated AISI 301 steel samples, that the open circuit potential (E_{ocp}) decrease along with increasing of deformation degree in cold rolling process. The obtained potential values changed in a range from the value -342 mV for the material as-delivered (undeformed state) to the value - 678 mV for a specimen with 80% of cold deformation. Given that the potential is determined by the ion exchange processes occurring between the test sample and the corrosion solution, so its lower values should be associated with the passivation ability of the steel in the corrosion medium, which deteriorates as the degree of cold deformation increases (Varga et al., 2001).

Polarization curves showing the dependence between voltage and current density were plotted for AISI 301 steel samples in the undeformed state and after cold deformation in the range of 30% to 80% (Fig.13).

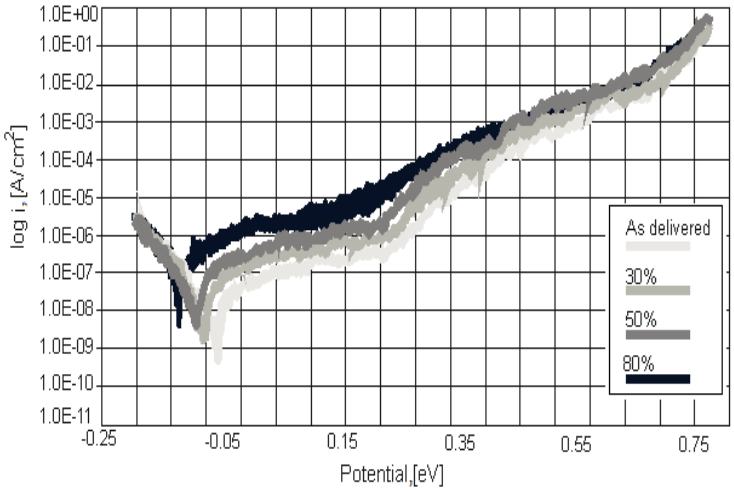

Fig. 13. Polarization curves determined in 0.5N NaCl solution for AISI 301 steel in delivery state and after selected rolling reductions

A similar shape of polarization characteristics was obtained for all investigated AISI 301 steel samples. In the cathodic range of the polarization curves, similar values of current density were found. However, in the anodic range of the polarization curves, a clear increase in current density values was observed with the degree of deformation. The analysis of the curves shows that there is a clear tendency to decrease the values of the cathode-anode transition potential and increase the values of the currents obtained for this potential as the material is strengthened by plastic deformation in cold rolling process. In the course of the curves, there is a clear loss of stability in the density of currents, associated with changes occurring in the passive layer of the material. With the degree of deformation these changes were observable at increasingly smaller potential values. The values of corrosion potential E_{cp} and corrosion current i_{cor} determined by extrapolation of the Tafels curves, have been presented in Table 3.

Table 3. Electrochemical results of AISI 301 steel

Degree of deformation, %	0%	30%	50%	80%
E_{cp} (mV)	-130	-219	-242	-268
i_{cor} ($\mu A/cm^2$)	0.35	7.31	8.53	9.71

On the basis of electrochemical tests of AISI 301 steel, it was found that the value of the corrosion potential for the undeformed sample was -130mV and decreased to a value of -268mV - for the sample with a maximum of 80% deformation. Such a value of the potential difference is sufficient for corrosion to occur, in case there are places in the material with such a different degree of deformation. The value of the corrosion current increased 28 times from 0.35 $\mu A/cm^2$ for undeformed sample (the material in the delivery state), to 9.71 $\mu A/cm^2$, for the material after maximum deformation. The obtained values of corrosion potential and corrosion current density in a chloride environment for austenitic Cr-Ni steels are also confirmed by studies given by other authors (Kumar et al. 2007, Zhilin et al. 2006, Rutkowska-Gorczyca et al., 2009, Silva et al., 2023). The changes in pitting potential that occur in deformed samples are the result of stresses caused by α'-martensite deformation or dislocations. The martensitic phase can not only cause a decrease in solution resistance in the pit, but also induce a decrease in polarization resistance between the metal and the pit. Therefore, accelerated pitting corrosion in cold-rolled Cr-Ni steel is accelerated with an increase in the volume fraction of martensite (Kamide et al., 1994).

The result of SEM observations of the samples surface after electrochemical corrosion testing in 0.5N NaCl revealed a similar type and degree of corrosion damage to that of the samples after corrosion testing in this environment, but using the weight method. The surface of AISI 301 steel in the undeformed state after electrochemical corrosion testing is characterized by relatively small and not very deep corrosion pits as well as a cracked surface layer (Fig.14).

Numerous micropores, corrosion pits and a cracked surface layer were observed on the surface of the specimens after deformation in the cold-rolling process, especially at the maximum (80%) degree of deformation (Fig.15). Obtained nature of corrosion pits was similar to the results given in work (Ernst and Newman, 2002), which also were carried out in the environment containing ions Cl^-. The corrosion pits observed on the AISI 301 steel surface

after 80% deformation and electrochemical testing in 0.5N NaCl were deeper than those obtained in the undeformed structure (Fig.14-15). Authors of work (Ernst and Newman, 2002) proved that pit growth in depth follows a parabolic law with time and is independent on the potential.

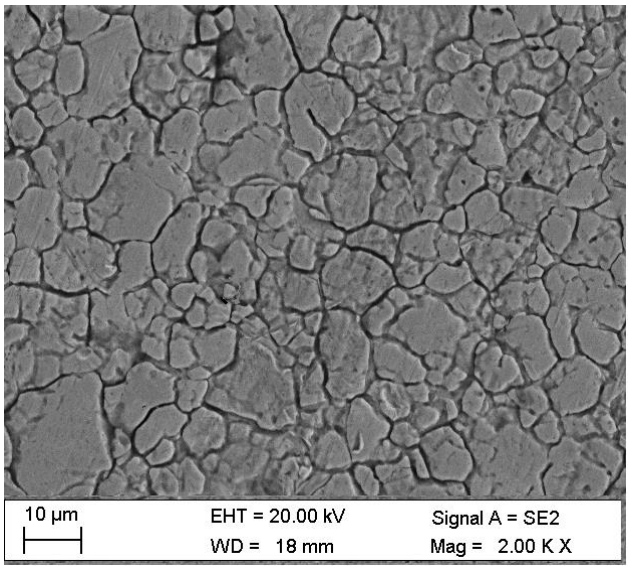

Fig. 14. Cracked surface layer and corrosion pits of the AISI 301 steel in a delivery state and electrochemically tested in 0.5N NaCl solution

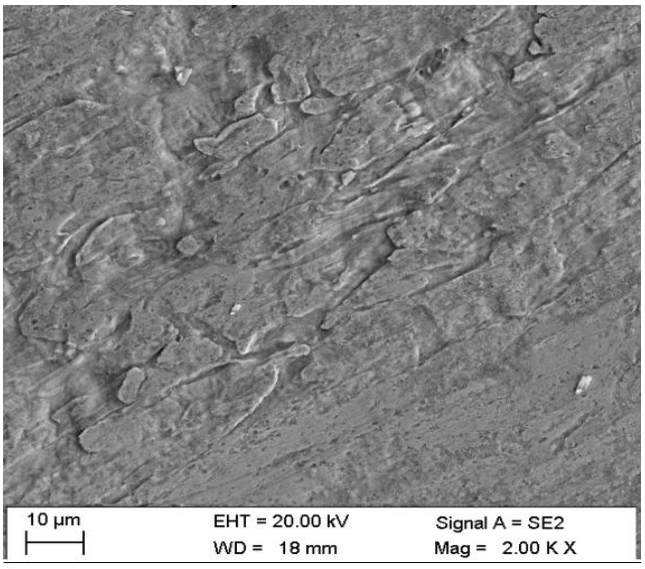

Fig. 15. Numerous corrosion pits on the surface of the AISI 301 steel 80% deformed and electrochemically tested in 0.5N NaCl

4. CONCLUSIONS

Metallographic investigations of samples cut from the AISI 301 sheet showed that the steel has a single-phase austenitic microstructure with numerous annealing twins as well as non-metallic inclusions. After plastic deformation in the range from 30% to 80% the martensite α' phase and shear bands were reveled in the microstructure of investigated steel. The presence of α'-martensite in the plastically deformed AISI 301 steel is confirmed by X-ray phase analysis. On the diffraction patterns of steel middle layers after 30% of cold rolling, there are disclosed three diffraction lines coming from planes (111)γ, (220)γ and (311)γ austenite phases and three (110)α', (200)α', (211)α' reflection planes from martensite-α' phases. It should be note, that on diffractogram were not disclosed diffraction lines coming from hexagonal close packed martensite - ε. This means that in this work the probably sequence of the martenisitic transformation is $\gamma \rightarrow \alpha'$.

Corrosion tests by gravimetric method showed that investigated steel is not resistant to corrosion in 0.5N H_2SO_4 solution, while no significant weight loss was observed in artificial seawater solution (0.5N NaCl). According the potentiodynamic tests carried out in 0.5N NaCl solution it was found that the increase of the degree of plastic deformation from 30% up to 80% results in lowering the corrosion potential as well as increases the values of corrosion current density resulting in a significant decrease in the steel resistance to pitting corrosion. Occurring this dependence is connected with appears of strain induced martensite-α' in deformed AISI 301 steel structure.

Conducted SEM analyses of samples after corrosion tests in both acidic and chloride environments revealed corrosion products on their surface in a form of pits with diversified size. Corrosion damages, in particular, pitting observed on the steel surface after plastic deformation in the range of 30% to 80% and immersion testing in 0.5N H_2SO_4 were more numerous and deeper than the pitting obtained under the same conditions but 0.5N NaCl environment. Damaging of a superficial layer has occurred around the pits. Moreover, cracked passivation layer after corrosion test in both environments, allowing further penetration of the corrosive medium was observed. Many studies have evidenced that the presence of high-density dislocations and numerous defects has an adverse effect on the metal materials' pitting corrosion resistance, not only increasing the pit generation rate (Varga et al., 2001, Zhilin et al., 2006, Silva et al., 2023), but also producing a more defective passive films.

REFERENCES

1.Abreu H., Carvalho S., Neto P., Santos R., Freire V., Silva P., Tavares S., (2007). *Deformation induced martensite in an AISI 301LN stainless steel: Characterization and influence on pitting corrosion resistance,* Mater. Res., 10(4), 359-366.

2.Azambuja D.S., Martini E.M., (2003). *Corrosion behaviour of iron and AISI 304 stainless steel in tungstate aqueous solutions containing chloride*, Journal of the Brazilian Chemical Society, 14, 570-576.
*3.*ASTM E407 - *Standard Practice for Microetching Metals and Alloys.*
*4.*ASTM G5 - *Potentiodynamic Anodic Polarization Measurements.*
5.Barbucci, A., Cerisola, G., Cabot, P.L., (2002). *Effect of cold working in the passive behavior of 304 stainless steel in sulfate media.* Journal of Electrochemical Society, 149, 534-542
6.Baszkiewicz J., Kamiński M., (1997). *Fundamentals of materials corrosion*, The Warsaw University of Technology Publishers, Warsaw (in Polish).
7.Blicharski M., (2004). *Materials engineering. Steel*, Scientific and Technical Publishers, Warsaw.
8.Calculation of pitting resistance equivalent numbers (PREN) – British Stainless Steel Association (bssa.org.uk), 2023.
9.Chunchun X., Gang H., (2004). *Effect of deformation-induced martensite on pit propagation behavior of 304 stainless steel*, Anti-Corrosion Methods and Materials, 51, 381-388.
10.Darowicki K., (2008). Corrosion Processes, Gdansk University of Technology.
11.Dobrzański L.A., (2009). *Shaping the structure and properties of engineering and biomedical material surfaces*, (in Polish), International OCSCO World Press, Gliwice, pp. 123-134.
12.Ernst, P., Newman R.C., (2002). Pit growth studies in stainless steel foils, I. Introduction and pit growth kinetics, Corrosion Science, 44, 927-941.
13.Ernst, P., Newman R.C., (2002). Pit growth studies in stainless steel foils, II. Efect of temperature, chloride concentration and sulphate addition, Corrosion Science, 44(5), 943-954.
14. Lamb S., Handbook of Stainless Steel and Nickel Alloys, CASTI Publishing INC./ASM International (2001).
15.Haušild P., Davydov V., Drahokoupil J., Landa M., Pilvin P., (2010). *Characterization of strain-induced martensitic transformation in a metastable austenitic stainless steel*, Mater. Design., 31, 1821-1827.
16.Garcia E.G.; Paniagua F.A.; Herrera-Hernández H.; Juárez Garcia J.M.; Pardavé M.E., Romo, M.A., (2010). *Electrochemical and microscopy study of localized corrosion on a sensitized stainless steel AISI 304.* ESC Transactions, 29(1), 93-102.
17.Kamide, H.; Fujitsuka, K.m Tanaka, Y., (1994). *Effect of carbon content on dissolution rate of α' martensite and 304 stainless steel in a H_2SO_4-NaCl solution*. Journal of the Japan Institute of Metals, 58, 1414-1419.
18.Kerner Z., Horváth A., Nagy G., (2007). *Comparative electrochemical study of 08H18N10T, AISI 304 and AISI 316L stainless stee*l, Electrochimica Acta, 52, 7529-7537.
19. Kumar, B.R., Mahato, B., Singh, R., (2007). *Influence of cold-worked structure on electrochemical properties of austenitic stainless steels*, Metallurgical and Materials Transactions, 38A, 2085-2094.
20.Lisiecki A., Kurc-Lisiecka A., Juroszek W., (2019). *Corrosion resistance of laser welded butt joints of austenitic steel sheets*, Steel, Metals & New Technologies, 5-6, 117-123.
21.Otero E., Pardo A., Sáenz E., Utrilla V., Pérez F., (1995). *Intergranular corrosion behaviour of a new austenitic stainless steel low in nickel*, Canadian Metallurgial Quarterly, 34, 135-141.
22.Ozgowicz W., Kurc-Lisiecka A., Grajcar A., (2012). *Corrosion Behaviour of cold-deformed austenitic alloys, In: Environmental and Industrial Corrosion- Practical and Theoretical Aspects*, B. Valdez, M. Schor (Ed.), 79-107, InTech, ISBN 978-953-51-0877-1, Rijeka, Croatia.
23.Pardo A., Merino M.C., Carboneras M., Coy A.E., (2007). *Pitting corrosion behaviour of austenitic stainless steels with Cu and Sn additions*, Corrosion Science, 49, 510-525.
24.Peğuet L., Malki B., Baroux B., (2007). *Influence of cold working on the pitting corrosion resistance of stainless steels*, Corrosion Science, 49, 1933-1948.
25.Rutkowska-Gorczyca, M., Podrez-Radziszewska, M., Kajtoch, J., (2009). *Influence of cold working process on the corrosion resistance of steel 316L*. SIM XXXVII, Kraków-Krynica, pp. 319-323.
26.Salomon N., Salomon I., (2010). *Phase transformation influence on corrosion resistance of AISI 316 austenitic stainless steel*, U.P.C.Sci., Bull., Series B, 72(4), 197-206.
27.Silva P.M.O.; Filho M.C.C., Cruz J.A.d.; Sales A.J.M.; Sombra A.S.B.; Tavares J.M.R.S., (2023). *Influence on Pitting Corrosion Resistance of AISI 301LN and 316L Stainless Steels Subjected to Cold-Induced Deformation*. Metals, 13, 443.
28.Sing V.B., Ray, M., (2007). *Effect of H_2SO_4 addition on the corrosion behaviour of AISI 304 austenitic stainless steel in methanol-HCl solution*. International Journal of Electrochemical Science, 2, 329-340.
29.Standard PN-EN ISO 7384 - *Corrosion tests in an artificial atmosphere - General requirements.*
30.Standard PN-EN ISO 8044 - *Corrosion of metals and alloys - Basic terms and definitions.*
31. Standard PN-EN ISO 3651-2 - *Determination of intergranular corrosion resistance of corrosion-resistant stels -- Part 2: Ferritic, austenitic and ferritic-austenitic (duplex) corrosion-resistant steels -- Corrosion test in an environment containing sulfuric acid (VI).*

*32.*Standard PN-H-04608 – *Corrosion of metals Scale of corrosion resistance of metals.*
33.Štefec, R., Franz F., (1978). *A study of the pitting corrosion of cold-worked stainless steel*. Corrosion Science, 18(2), 161-168.
34.Varga K., Baradlai P., Hirschberg G., Nemeth Z., Oravetz D., Schunk J., Tilky P., (2001). *Corrosion behaviour of stainless steel surfaces formed upon chemical decontamination*, Electrochim. Acta, 46, 3783-3790.
35.Zhilin, L., Wei, L., Juncai Q., (2006). *The effect of electrochemically induced annealing on the pitting resistance of metastable austenitic stainless steel*, Metallurgical and Materials Transactions, 37A(2), 435-439.

Received: May 12, 2023/ Accepted: December 15, 2023 / Paper available online: December 20, 2023© International Journal of Modern Manucaturing Technologies